

Improvement in Hot-Metal Dephosphorization

Naoto SASAKI*
Susumu MUKAWA

Yuji OGAWA
Ken-ichiro MIYAMOTO

Abstract

The converter-type hot metal pretreatment process which is developed and installed by NSC for all works is marked for improved productivity, heat balance and reduction of amount of slag without fluorine. The improvement is realized by lower basicity and higher oxygen potential. This report describes 1) the behavior of dephosphorization with lower basicity slag, 2) the evaluation and improvement of oxygen potential at the interface of slag and metal, 3) the improvement of dephosphorization reaction by using solid phase which is contain high phosphorous. The idea and feature of the MURC (Multi-Refining Converter) method and effects of implement of the converter- type hot metal pretreatment process are described.

1. Introduction

Nippon Steel Corporation has long since focused on hot-metal pretreatment as an effective measure to produce ultra-low-P steels and to improve steel refining efficiency to reduce costs. Conventional hot-metal pretreatment methods using torpedo ladle cars or molten metal ladles as the reaction vessels enabled stable production of low-P, low-S steels, but it required desiliconization at a prior stage, and as a result, the thermal allowance for the decarburization in converters decreased and the scrap ratio was significantly restricted. As a solution, Nippon Steel Corporation's Nagoya Works developed the LD converter-optimized refining process (LD-ORP),¹⁻³⁾ whereby Si and P were sequentially removed from hot metal in one converter. The new process was put into commercial practice, and is now also used at Yawata and Kimitsu Works for producing ultra-low-P steels. More details on LD-ORP are given in another article of this issue.⁴⁾

Nippon Steel Corporation developed another method of hot-metal pretreatment using converters: the multirefining converter (MURC) process, whereby hot metal is dephosphorized and decarburized sequentially in the same converter vessel with deslagging in between.⁵⁻⁹⁾ This process does not require vessel change after dephosphorization, and thus allows steel refining at minimum heat loss because of hot recycling of the slag formed during decarburization for the following charge, internally called "inverse-slag-flow refining." In appreciation of this, after its development at Muroran Works, originally for producing ordinary carbon steels except for ultra-low-P steels, and improvements at Oita Works to reduce process time, etc.,¹⁰⁻¹⁴⁾ MURC was introduced to Kimitsu and Yawata for wide applications. This unique process is presented in more

detail in the following sections.

The converter-type hot-metal dephosphorization uses a large freeboard, ample oxygen-blowing capacity, and metal bath stirring by bottom gas blowing of converters, and thus is advantageous in terms of thermal allowance and processing time. Dephosphorization using converters expanded further when regulations on fluorine discharge were set forth in 2001. By the hot-metal pretreatment in torpedo ladle cars (TPC-ORP), which uses highly basic slag, the dephosphorization efficiency falls significantly without the use of fluorine. In converters, in contrast, high oxygen potential is maintained because of oxygen blowing at high speed, and dephosphorization progresses even with slag of low basicity (CaO/SiO_2), and thus the use of fluorine is not absolutely necessary.

As a result of the rapid development and expansion of hot-metal pretreatment making use of the advantages of converters since the 1990s, 95% of the molten pig iron of the company undergoes the converter-type dephosphorization as of early 2012.¹⁵⁾

This paper reports the evaluation of the dephosphorization characteristics of low-basicity slag, fundamental studies on the interface oxygen potential, and the study results of the role of the solid phase in slag in dephosphorization reactions. Also presented herein are the changes in reaction characteristics caused by the introduction of the converter-type hot-metal dephosphorization at some of the steel-making plants of the company.

2. Development of MURC Process⁵⁾

By LD-ORP, dephosphorization and decarburization are conducted in different converter vessels. The MURC process was de-

* Senior Researcher, Steelmaking R&D Div., Process Technology Center 20-1 Shintomi, Futtsu, Chiba 293-8511

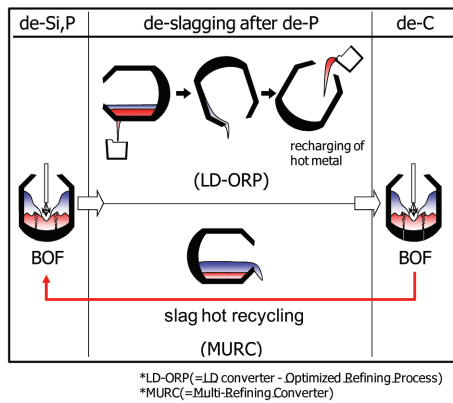


Fig. 1 Converter-type hot metal pretreatment processes at Nippon Steel Corporation¹⁶⁾

veloped to make the vessel change unnecessary: after dephosphorization, slag is discharged by tilting the converter, and then decarburization is conducted in the same vessel. The advantages of the process, besides those of the converter-type pretreatment, are that the loss of time and heat due to vessel change is avoided, and that decarburization slag can be left in the vessel and used for the following charge, which lowers lime consumption (Fig. 1¹⁶⁾). The tests conducted during the development stage using a laboratory converter are outlined in the following subsections.

2.1 Experimental procedure

Tests were conducted using an 8-t laboratory converter. Dephosphorization tests were conducted changing the mixing ratio of top and bottom blowing and the slag basicity in terms of the CaO/SiO_2 . L/L_0 (the ratio of the depth of the cavity formed by top-blown oxygen L ¹⁷⁾ to the metal bath depth L_0), an index of the intensity of stirring during dephosphorization, was changed in a range of 0.02-0.42 around a standard value of approximately 0.05. Nitrogen was blown from the bottom, and the power density¹⁸⁾ of the stirring by bottom blowing was changed from about 1.6 to 3.6 kW/t. The dephosphorization flux was composed only of iron ore and burnt lime, and the range of its basicity was changed within a range from 0.9 to 2.2.

2.2 Result and discussion

A Healy-type¹⁹⁾ equation, equation (1), for estimating the phosphorus distribution in metal and slag was obtained through multiple regression using the steel chemistry and temperature at the blow ends of dephosphorization and decarburization. Here, as the basicity components of the slag, only CaO and MgO were considered, and in consideration of the difference in the C concentration in metal after dephosphorization and decarburization, a parameter of interaction between P and C was introduced.²⁰⁾

$$\log (\%P) / [\%P] = 2.5 \log (\%T.Fe) + 0.0715 \{ (\%CaO) + 0.25 (\%MgO) \} + 7710.2/T - 8.55 + (105.1/T + 0.0723) [\%C], \quad (1)$$

where (%P) is the P concentration in slag, [%P] is the same in metal, (%T.Fe) is the total Fe concentration in slag, (%CaO) and (%MgO) are the respective concentrations in slag, T is the metal temperature at the end of dephosphorization (K), and [%C] is the C concentration in metal (all percentages are in mass).

Fig. 2 shows the relationship between (%T.Fe) and the phosphorus distribution ($(\%P)/[\%P]$) calculated using the equation for the cases of the slag basicity of 1.0, 1.5, and 2.0. For the calculation, the temperature was assumed to be 1,350°C, the C concentration in metal 3.5 mass%, the MgO concentration in slag 5 mass%, and the contents of MnO and other trace components 15 mass% in total.

Note that the graph includes those test results where the slag basicity was close to 1.0, 1.5, or 2.0; the figures were corrected to match the conditions of 1,350°C and 3.5 mass% C in metal. The graph shows good agreement of the calculated figures with the corrected test results. The ratio $(P)/[P]$ near 100 in the slag basicity range of 1.0 to 1.5 indicates that effective dephosphorization is possible even when slag basicity is low. However, when (%T.Fe) is excessively high, $(P)/[P]$ decreases owing to dilution of basicity components. In dephosphorization with low-basicity slag, as in the present study, therefore, the adequate range of the total Fe concentration in slag after the processing is 15 to 25 mass%.

A significant advantage of MURC is that all the slag of decarburization can be left in the converter vessel and effectively used for the dephosphorization of the following charge. Fig. 3 shows the relationship between the unit consumption of the burnt lime added during desiliconization and dephosphorization and the P concentration in metal $[P]$ after dephosphorization. With slag recycling, burnt lime consumption decreases by 5 to 10 kg/t.

As described above, the tests confirmed that good dephosphorization is possible even with low-basicity slag, and that the recycling of decarburization slag significantly decreases the lime consumption and slag discharge.

After the above tests, the MURC process was tested and evaluated at Steelmaking Plant of Muroran Works, and then put into commercial practice there for the first time.⁶⁻⁹⁾

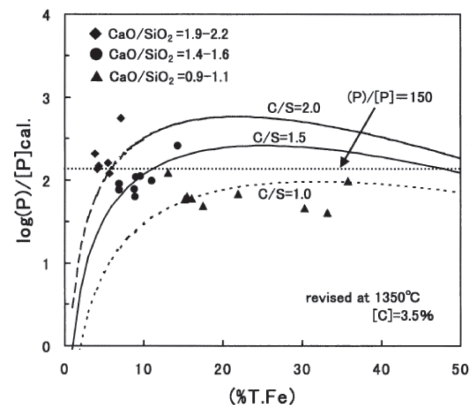


Fig. 2 Influence of slag composition on $(P)/[P]$ ratio⁵⁾

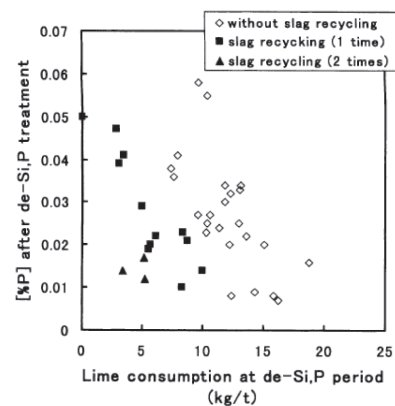


Fig. 3 Effect of slag recycling on lime consumption⁵⁾

3. Dephosphorization Characteristics with Low-basicity Slag^{21, 22)}

Intensive stirring of the metal bath to accelerate mass transfer is expected to be effective at accelerating dephosphorization reactions. However, increasing only the stirring energy accelerates the FeO reduction in the slag, making its concentration too low, and leads to a decrease in interface oxygen activity, an increase in the slag resistance to material transfer, and consequently a decrease in the dephosphorization rate. On the other hand, as long as the metal bath stirring is weak, if the rate of oxygen blowing is increased, dephosphorization will not be accelerated because the reaction rate will be governed by the mass transfer rate of phosphorus in the metal bath. Therefore, there must be a certain optimum relationship between the bath stirring energy by bottom blowing and the oxygen supply.

3.1 Experimental procedure

Dephosphorization tests were carried out using a commercially operating converter of Nagoya Works equipped with bottom blowing facilities for powder injection.^{23, 24)} Burnt lime, iron ore, and fluorspar were added to approximately 110 t of molten pig iron, and the amount of top blown oxygen was changed. Either lime stone or burnt lime, together with nitrogen gas, was blown in through two bottom tuyeres. The stirring energy was changed by controlling the flow rate of bottom-blown nitrogen or the amount of lime stone powder, which would thermally decompose and generate carbon dioxide gas.

3.2 Result and discussion

Fig. 4 shows the effects of the total oxygen blowing rate V_{O_2} ($Nm^3/t \cdot min$) and the stirring energy density of bottom blowing ε' (kW/t)¹⁸⁾ over the dephosphorization rate k_p' , which is defined as a macroscopic parameter by equation (2).

$$k_p' = \{ \ln ([\%P]_i / [\%P]_f) \} / t, \quad (2)$$

where $[\%P]_i$ and $[\%P]_f$ are the P concentrations (mass%) in the molten metal before and after the reaction, respectively, and t is time.

Macroscopically speaking, k_p' increases when V_{O_2} and ε' are increased simultaneously. When ε' is increased to 4 kW/t or more, k_p' increases with increasing V_{O_2} . As far as the present tests are concerned, a maximum k_p' value of 0.33 min^{-1} was obtained when V_{O_2} was 2.8 $Nm^3/t \cdot min$ and ε' was 15 kW/t ; the dephosphorization time under this condition was 5.2 min. The solid lines in the graph are expected iso- k_p' curves (of the same dephosphorization rate) based on a coupled reaction model.²⁵⁾ When ε' was excessively large in a

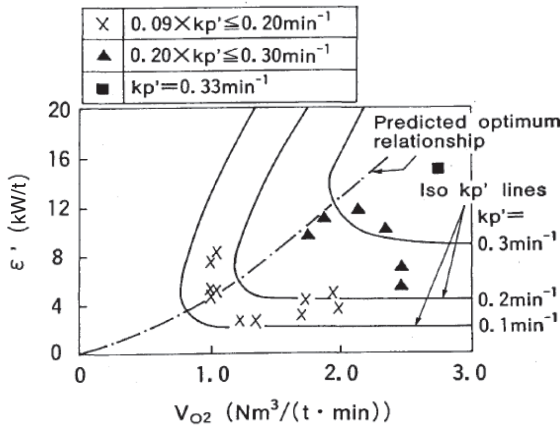


Fig. 4 Influence of stirring energy for molten bath and rate of supplied oxygen on dephosphorisation rate²¹⁾

range of low V_{O_2} , for instance, $V_{O_2} = 1 Nm^3/t \cdot min$ and $\varepsilon' = 20 kW/t$, then slag became over-reduced. In contrast, when V_{O_2} was excessively large in a range of low ε' , such as $V_{O_2} = 3 Nm^3/t \cdot min$ and $\varepsilon' = 4 kW/t$, then the reaction rate was governed by the transfer rate of P in the metal bath. As explained here, k_p' does not increase when either V_{O_2} or ε' alone is increased. Therefore, to accelerate the dephosphorization reaction in commercial operation, it is desirable to intensify the stirring force by bottom bubbling and control the oxygen supply within an adequate range, since decarburization suppression is sometimes required and the loss of hot metal by oxidation should be minimized.

4. Evaluation of Oxygen Potential at Slag/Metal Interface²⁶⁾

By converter-type hot-metal pretreatment, it is possible to dephosphorize molten pig iron using low-basicity and high-oxygen-potential slag. The oxygen potential at the reaction interface constitutes an important factor for high reaction efficiency. Nevertheless, there have been very few studies on the composition of the slag used for the process. In consideration of the situation, the authors studied the effects of slag composition by employing the method of estimating the interface oxygen potential from the compositions of the metal and slag at the time when dephosphorization ends and rephosphorization begins.

4.1 Experimental procedure

Carbon-saturated molten pig iron (70 kg) containing roughly 0.1 mass% P was melted in a high-frequency furnace, and held at 1,350°C. The slag of CaO-SiO₂ was added to it by 20 kg/t-iron, and then melted. Then, under stirring by bottom blowing of Ar, iron oxide was added to the molten pig iron as an oxygen source for dephosphorization to take place; the iron oxide was added in 40 doses at intervals of 1 min to a total oxygen supply of 8 Nm^3/t -iron. Then, after stopping the iron oxide addition, the Ar bottom blowing was continued for 20 min so for rephosphorization to occur.

4.2 Result and discussion

According to Pan et al.,²⁷⁾ the left-hand side of equation (3) is zero at the time (t) of the change from dephosphorization to rephosphorization, and therefore, equation (4) holds true. Assuming that the interface is in equilibrium at time t , the oxygen potential at the interface $P_{O_2}^*$ is expressed by equation (5) using actually measured distribution of P.

$$-d[\%P]/dt = k_m \frac{A}{V_m} \{ [\%P] - [\%P]^* \} = k_s \frac{A}{V_s} \{ (\%P)_i - (\%P) \} \quad (3)$$

$$[\%P] = [\%P]_i = [\%P]^*, \quad (\%P) = (\%P)_i = (\%P)^* \quad (4)$$

$$P_{O_2}^* = (95K/31)^{4/5} \times (C_{PO_4})^{-4/5} \times \{ [\%P]_i / [\%P]_i / f_p \}^{4/5} \quad (5)$$

where K is the equilibrium constant for $1/2 P_2 = P$; A is the area of the reaction interface (m^2); k_m and k_s are the material transfer coefficients in the metal and slag, respectively (m/s); V_m and V_s are the volumes of the metal and slag, respectively (m^3); $[\%P]_i$ is the P concentration in the metal bulk at time t (mass %); $(\%P)_i$ is the P concentration in the slag bulk at time t (mass %); $[P]^*$ and $(P)^*$ are the P concentrations on the metal side and slag side, respectively, at the interface (mass%); C_{PO_4} is the phosphate capacity of the slag; and f_p is the activity coefficient of P in the metal (per 1 mass%).

An example of the test results is shown in Fig. 5. The graph clearly shows that dephosphorization advances while iron ore is added, but after the end of its addition, the reaction turns to rephosphorization. The graph of Fig. 6 is obtained by calculating interface oxygen potentials for different slag compositions from the test re-

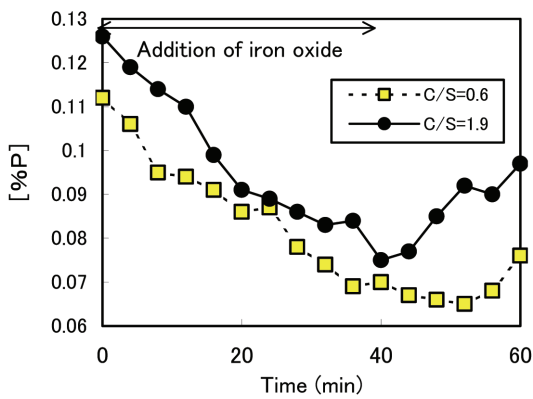


Fig. 5 Behavior of [%P] during experiment²⁶⁾

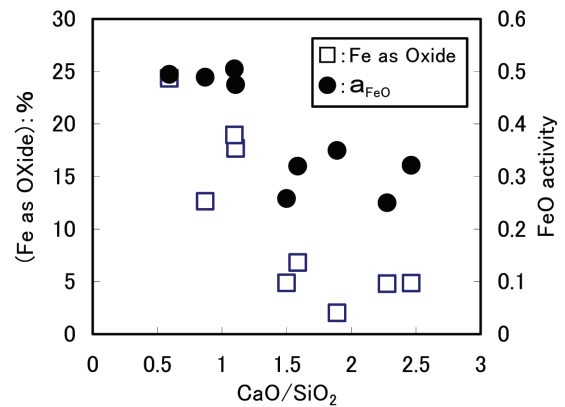


Fig. 7 Effect of CaO/SiO₂ on (%Fe as oxide) and a_{FeO}²⁶⁾

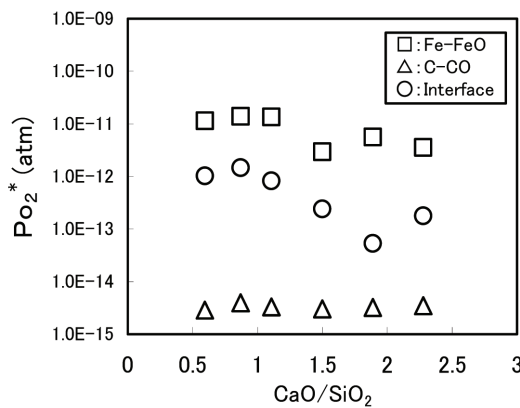


Fig. 6 Relationship between CaO/SiO₂ and P_{O₂}²⁶⁾

sults, following the method through which equation (5) was derived. The interface oxygen potential lies between the oxygen potential of the slag bulk, which is defined by the Fe-FeO equilibrium, and the same of the metal bulk, which is defined by the C-CO equilibrium. However, when basicity is higher than 1.5, it falls rapidly to approach the oxygen potential of the metal bulk. Fig. 7 shows the relationship between slag basicity (CaO/SiO₂) and iron oxide concentration and FeO activity under an assumption that the interface is in equilibrium; FeO activity was obtained from the slag composition at the time of measurement by computational thermodynamics.²⁸⁾ While iron oxide concentration decreases with increasing basicity, FeO activity remains substantially unchanged within either the low- or high-basicity range.

However, the level of FeO activity is markedly low in the range where CaO/SiO₂ is about 1.5 or more, which leads to the fall of the interface oxygen potential. If it is possible to raise the interface oxygen potential closer to the potential in the slag bulk, determined by the Fe-FeO equilibrium, it will be possible to further accelerate dephosphorization. On the other hand, the interface oxygen potential is close to the potential in the slag bulk in the range where CaO/SiO₂ is comparatively low. This indicates that effective dephosphorization is possible even when slag basicity is low.

5. Study on Effects of Solid Phase in Slag over Dephosphorization Reactions²⁹⁾

The enactment of the regulations on the discharge of fluorine

into the environment has made it necessary to decrease slag formation through higher dephosphorization efficiency and eliminate the use of fluorspar. The slag that forms during dephosphorization is mostly multiphase slag comprising both solid and liquid, and considering the effects of the solid phase is very important in clarifying the mechanisms of dephosphorization reactions. In view of the situation, the authors conducted dephosphorization tests changing the composition of the solid phase in the slag that forms during the reaction, and examined the relationship between the type of the solid phase and dephosphorization efficiency.

5.1 Experimental procedure

A graphite crucible was placed in a high-frequency melting furnace, a MgO crucible was placed inside the graphite crucible, and 600 g of pig iron containing 4.0 mass% C and 0.1 mass% P was melted at 1,400°C in the MgO crucible, using the graphite crucible as the heating element. Here, the initial Si content of the pig iron was changed from charge to charge. Then, flux powder, which was prepared separately by mixing, melting, and crushing industrial burnt lime and iron ore, was added to the molten iron in three doses, 10 g each, at intervals of 2 min. The samples after the processing were left to cool slowly in the crucibles. Slag samples were taken from some charges, embedded in resin, cut, polished, and coated at the section surface with carbon by vapor deposition, and submitted to EPMA analysis.

5.2 Result and discussion

Fig. 8 shows the relationship between the decrease in the silicon content $\Delta[\text{Si}]$ during the test and the dephosphorization efficiency of burnt lime $\eta_{\text{CaO}}^{\text{P}}$, which is defined by equation (6). Here, $\eta_{\text{CaO}}^{\text{P}}$ is an indicator of the ratio of CaO that takes part in the dephosphorization reactions in the form of $3\text{CaO} \cdot \text{P}_2\text{O}_5$ to the total CaO input.

$$\eta_{\text{CaO}}^{\text{P}} (\%) = \{ (3M_{\text{CaO}} \times \Delta[\%P] / 100) / (2M_{\text{P}}) \} / (W_{\text{CaO}} / 1000) \times 100 \quad (6)$$

where M_{CaO} is the molecular weight of CaO, W_{CaO} is the unit consumption of burnt lime (kg/t), $\Delta[\%P]$ is the decrease in P content (mass %), and M_{P} is the atomic weight of P.

The two solid lines in the graph indicate the linear regression of the points near $\Delta[\text{Si}] = 0.15$ mass% and that of the other points. Each of these lines fall monotonously because FeO is used for oxidation of Si, and CaO for the formation of complex oxides with silicates, and consequently, the dephosphorization efficiency of burnt lime decreases as desilicization advances. However, through comparison of the points near $\Delta[\text{Si}] = 0.15$ mass% with the others, it is clear that $\eta_{\text{CaO}}^{\text{P}}$ does not decrease monotonously but has local

maxima near $\Delta[\text{Si}] = 0.15$ mass% (point III and others nearby). The value of $\eta_{\text{CaO}}^{\text{P}}$ in this zone is roughly 15%, substantially at the same level of dephosphorization efficiency in a high basicity range of $[\text{Si}]_i < 0.005$ mass%.

Typical results of the mineralogical analysis by EPMA of the slag samples are given in Fig. 9. The upper frames of parts I to IV are the secondary electron images of the slag samples corresponding to points I to IV in Fig. 8, and the lower frames are presumed from respective characteristic X-ray images.

Here, in the range of $\Delta[\text{Si}]$ from 0.13 to 0.17 mass%, represented by point III, P is solute in CaO and SiO₂, and no free-CaO was found. According to the phase diagram, the crystallizing phase in this zone is 2CaO · SiO₂; this solid phase can contribute to the dephosphorization reactions because it can dissolve P in the form of

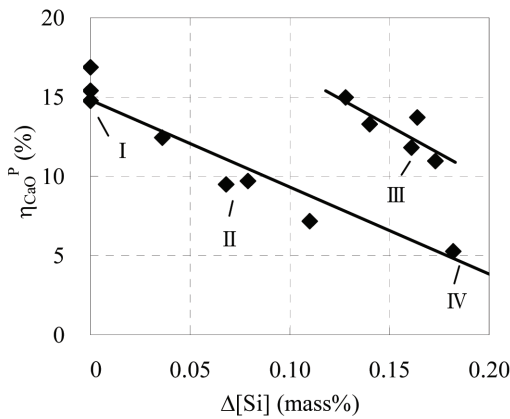


Fig. 8 Relationship between $\Delta[\text{Si}]$ and $\eta_{\text{CaO}}^{\text{P}}$ ²⁹⁾

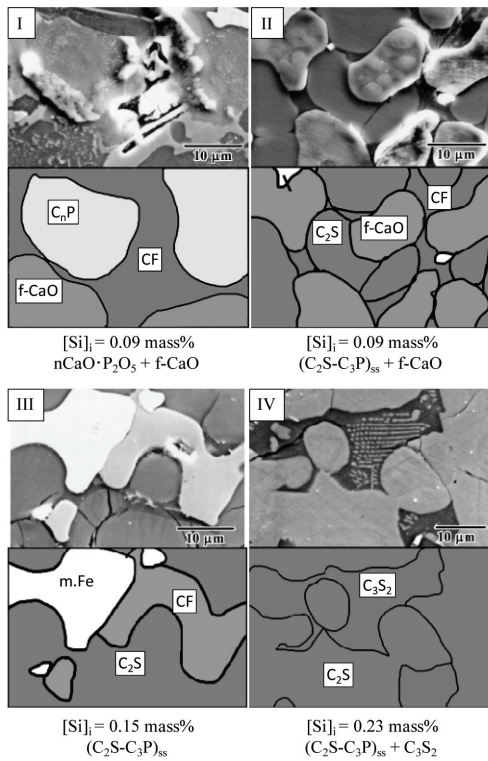


Fig. 9 Electron scanning image of the slag²⁹⁾

solute $3\text{CaO} \cdot \text{P}_2\text{O}_5$ over the full range of relative concentration.³⁰⁾ This indicates that, even when there is a solid phase in slag, P is condensed in this phase and the P concentration in the liquid phase is kept low, and as a result, high dephosphorization efficiency is obtainable even when the equilibrium P distribution of the liquid phase is comparatively low.

It is in the slag composition range where the basicity is 1.5 or more, on a comparatively high basicity side for hot-metal dephosphorization, that $2\text{CaO} \cdot \text{SiO}_2$ exists in steelmaking slag. When it is necessary to minimize the P content in hot metal, typically in the case of smelting low-P steel by LD-ORP, high-efficiency dephosphorization is possible by actively using the ability of the solid phase $2\text{CaO} \cdot \text{SiO}_2$ to condense P.

6. Expansion of Converter-type Hot-Metal Pretreatment Methods to Different Works³¹⁾

As explained above, converter-type hot-metal dephosphorization is greatly effective at coping with environmental regulations, increasing thermal allowance, and enhancing reaction efficiency. In appreciation of these advantages, various steel works of Nippon Steel Corporation have introduced the process, applied it to wider variety of steels, and added improvements to it. The results of the expansion of the LD-ORP and MURC processes to Yawata and Oita Works are presented in the following subsections.

6.1 Effects of LD-ORP at Yawata Works

Fig. 10 shows the relationship between CaO/O and the dephosphorization reaction efficiency of lime K_{CaO} by LD-ORP at Yawata Works in comparison with the same by the conventional TPC-ORP; CaO/O and K_{CaO} are given by equations (7) and (8), respectively. Note here that the dephosphorization reaction efficiency K_{CaO} is a standardized reaction efficiency assuming a first-order reaction (whose rate changes in proportion to the concentration of the reactant), and accordingly, the difference in initial P concentration is compensated.

$$\text{CaO} / \text{O} = W_{\text{CaO}} / W_{\text{O}} \quad (7)$$

$$K_{\text{CaO}} = \{ \ln ([\%P]_i / [\%P]_f) \} / W_{\text{CaO}} \quad (8)$$

where W_{CaO} is the unit consumption of CaO (kg/t); W_{O} is the unit consumption of oxygen (kg/t); and $[\%P]_i$ and $[\%P]_f$ are the P concentration (mass %) in molten metal before and after the processing, respectively.

Because LD-ORP enabled use of basicity slag lower than that for the old TPC-ORP, high dephosphorization efficiency of lime is maintained without requiring fluorspar.

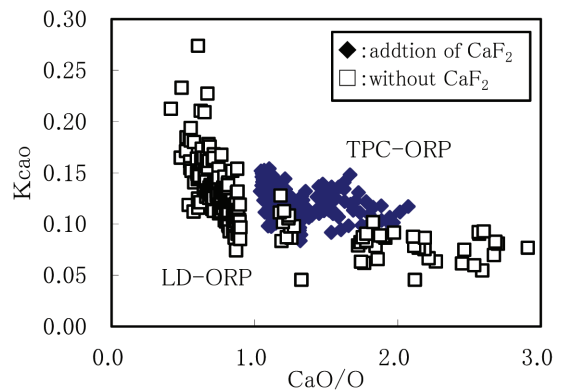


Fig. 10 Relationship between CaO/O and K_{CaO} (Yawata Works)³¹⁾

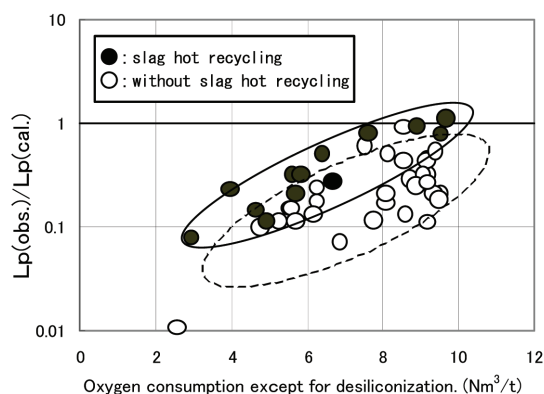


Fig. 11 Effect of slag hot recycling by MURC process (Oita Works)³¹⁾

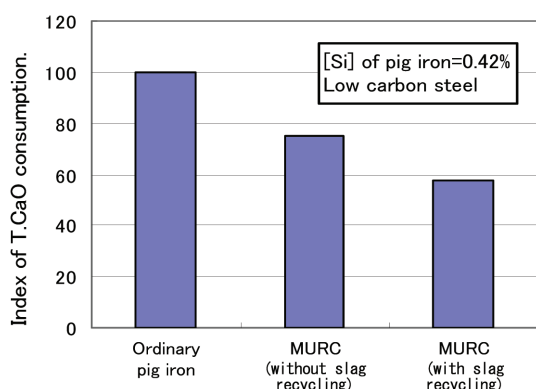


Fig. 12 Comparison of CaO consumption (Oita Works)³¹⁾

6.2 Introduction of MURC process at Oita Works

Fig. 11 shows the ratio between the phosphorus distribution (%P)/[P] actually measured at Oita Works, $L_p(\text{obs.})$ along the ordinate, and that calculated from the slag composition using equation (1), $L_p(\text{cal.})$, in two cases: one where decarburization slag is recycled in hot and the other where it is not. The graph shows that the slag hot recycling raised the phosphorus distribution to a level higher and closer to the calculated distribution, and decreased the lime consumption by an amount corresponding to the excess basicity of the hot-recycled slag (Fig. 12).

7. Summary

As described above, Nippon Steel Corporation developed converter-type hot-metal pretreatment processes, and expanded them to all steel works to enjoy the advantages of high productivity, wide thermal allowance, elimination of fluorine use, and reduction of slag formation.

Following the development of LD-ORP at Nagoya Works, the MURC process, whereby dephosphorization and decarburization are performed sequentially in one converter, was developed and spread to other works. The following results were obtained through the tests for the development of MURC using an 8-t laboratory converter:

(1) An equation for estimating the distribution of P between metal and slag was worked out, and it became clear that satisfactory dephosphorization was possible even with low-basicity slag when total Fe concentration in slag (%T.Fe) was kept within an

adequate range.

(2) Unit consumption of burnt lime was lowered by 5 to 10 kg/t as a result of reuse of decarburization slag for the dephosphorization of the following charge, and slag discharge was greatly decreased.

In addition, to establish high-efficiency dephosphorization practice for the converter-type hot-metal pretreatment, reaction kinetic studies were conducted using commercially operated converters, and the following became clear:

(3) Through tests of hot-metal dephosphorization and analysis using a competitive reaction model, it became clear that increasing the force for stirring the metal bath and the oxygen blowing rate in an adequate proportion to each other was effective at raising dephosphorization rate.

Furthermore, as the factors influencing dephosphorization reactions, the oxygen potential at the slag/metal interface and the relationship between the kind of solid phase in slag and the dephosphorization efficiency were examined, and the following findings were obtained:

(4) The oxygen potential at the slag/metal interface, which is normally somewhere between those in the slag bulk and metal bulk, falls markedly near the oxygen potential in the metal bulk when slag basicity is over 1.5.

(5) As a result of mineralogical analysis of slag, it was found likely that a $2\text{CaO} \cdot \text{SiO}_2$ phase capable of fixing P existed in regions where dephosphorization efficiency was high. Dephosphorization efficiency is presumed to increase when P condenses in the $2\text{CaO} \cdot \text{SiO}_2$ phase, and the P concentration in the liquid phase decreases as a result.

In contrast to the conventional TPC-ORP requiring high-basicity slag, the MURC process, which is applied mainly to ordinary carbon steels, actively lowers slag basicity, taking advantage of the high oxygen potential of converters, and improves thermal allowance and the dephosphorization efficiency of lime by recycling decarburization slag in hot for dephosphorization of the following charge.

By LD-ORP, on the other hand, even when it is used for heavy dephosphorization of hot metal for production of low-P steels, high-efficiency processing is possible without using fluorine. Even when slag basicity is comparatively high, P condenses in the solid $2\text{CaO} \cdot \text{SiO}_2$ phase, effectively contributing to high process efficiency.^{32, 33)}

In pursuit of higher steel refining efficiency, Nippon Steel Corporation aims at achieving 100% hot-metal pretreatment in 2013.¹⁵⁾

References

- 1) Katoh, K. et al.: CAMP-ISIJ. 4, 1153 (1991)
- 2) Katoh, K. et al.: CAMP-ISIJ. 4, 1154 (1991)
- 3) Nippon Steel's Nagoya Works: 104th Meeting of Steelmaking Committee of the Iron and Steel Institute of Japan. 1991 (for members only)
- 4) Fukuda, Y. et al.: Shinnittetsu Giho. (394), 91 (2012)
- 5) Ogawa, Y. et al.: Tetsu-to-Hagané. 87, 21 (2001)
- 6) Hayashi, H. et al.: CAMP-ISIJ. 15, 139 (2002)
- 7) Nippon Steel's Muroran Works: 125th Meeting of Steelmaking Committee of the Iron and Steel Institute of Japan. 2001 (for members only)
- 8) Nomata, H. et al.: Proc. 4th European Oxygen Steelmaking Conference. 2003, p. 79
- 9) Kobayashi, M. et al.: Shinnittetsu Giho. (394), 119 (2012)
- 10) Nippon Steel's Oita Works: 127th Meeting of Steelmaking Committee of the Iron and Steel Institute of Japan. 2002 (for members only)
- 11) Kume, K. et al.: CAMP-ISIJ. 16, 116 (2003)
- 12) Washizu, T. et al.: Proc. 1st Australia-China-Japan Symposium on Iron and Steelmaking. 2006, p. 188

NIPPON STEEL TECHNICAL REPORT No. 104 AUGUST 2013

- 13) Nippon Steel's Oita Works: 136th Meeting of Steelmaking Committee of the Iron and Steel Institute of Japan. 2007 (for members only)
- 14) Hashimoto, H. et al.: Shinnittetsu Giho. (394), 84 (2012)
- 15) Kumakura, M.: Shinnittetsu Giho. (394), 4 (2012)
- 16) Iwasaki, M. et al.: Shinnittetsu Giho. (391), 88 (2011)
- 17) Segawa, K.: Tetsu Yakin Hannou Kogaku (Iron Metallurgical Reaction Engineering). Tokyo, Nikkan Kogyo Shimbun, Ltd., 1977
- 18) Mori, K. et al.: Tetsu-to-Hagané. 67, 672 (1981)
- 19) Healy, G. W.: J. Iron Steel Ints. 208, 664 (1970)
- 20) Tsukihashi, F. et al.: Tetsu-to-Hagané. 76, 1664 (1990)
- 21) Mukawa, S. et al.: Tetsu-to-Hagané. 80, 207 (1994)
- 22) Mukawa, S. et al.: ISIJ-Int. 35, 1374 (1995)
- 23) Mori, M. et al.: Tetsu-to-Hagané. 72, S171 (1986)
- 24) Yoshida, S. et al.: Tetsu-to-Hagané. 72, S172 (1986)
- 25) Ohguchi, S. et al.: Ironmaking and Steelmaking. 11, 202 (1984)
- 26) Miyamoto, K. et al.: Tetsu-to-Hagané. 95, 199 (2009)
- 27) Han, M. et al.: Tetsu-to-Hagané. 76, 1488 (1990)
- 28) Yamada, W. et al.: Shinnittetsu Giho. (342), 38 (1991)
- 29) Sasaki, N. et al.: Tetsu-to-Hagané. 88, 300 (2002)
- 30) Fix, W. et al.: J. Am. Ceram. Soc. 52, 347 (1969)
- 31) Miyamoto, K. et al.: CAMP-ISIJ. 17, 642 (2004)
- 32) Mukawa, S.: Seikou Slag Kyokushouka ni muketeno Kaihatu Doukou to Kadai (Trend and Problems in Technical Development for Minimizing Steelmaking Slag). The Iron and Steel Institute of Japan, 1999, p. 57
- 33) Nippon Steel's Nagoya Works: 145th Meeting of Steelmaking Committee of the Iron and Steel Institute of Japan. 1991 (for members only)



Naoto SASAKI
Senior Researcher
Steelmaking R&D Div.
Process Technology Center
20-1 Shintomi, Futtsu, Chiba 293-8511



Yuji OGAWA
Chief Researcher, Dr.Eng.
Steelmaking R&D Div.
Process Technology Center



Susumu MUKAWA
Chief Researcher, Dr.Eng.
Nagoya R&D Lab.



Ken-ichiro MIYAMOTO
Senior Researcher, Dr.Eng.
Muroran R&D Lab.